

Geophysical Research Letters

RESEARCH LETTER

10.1029/2018GL080744

Key Points:

- Robust atmospheric mesoscale signals are embedded within basin-scale NAO variability in the western North Atlantic
- This mesoscale variability might be a response to changes in the temperature and velocity structure of the Gulf Stream driven by the NAO
- Study examines the new high-resolution ERA5 atmospheric reanalysis

Supporting Information:

- Supporting Information S1
- Figure S1

Correspondence to:

A. Cobb,
a.cobb15@imperial.ac.uk

Citation:

Cobb, A., & Czaja, A. (2019). Mesoscale signature of the North Atlantic Oscillation and its interaction with the ocean. *Geophysical Research Letters*, 46, 5575–5581. <https://doi.org/10.1029/2018GL080744>



Received 3 OCT 2018

Accepted 22 APR 2019

Accepted article online 29 APR 2019

Published online 21 MAY 2019

Mesoscale Signature of the North Atlantic Oscillation and Its Interaction With the Ocean

A. Cobb¹  and A. Czaja¹ 

¹Department of Physics, Imperial College London, London, UK

Abstract This observational study uses high-resolution data to investigate mesoscale signatures of the North Atlantic Oscillation (NAO) in the atmosphere and ocean. The production of spatially high-pass (“mesoscale”) filtered kinetic energy by buoyancy and shear effects in the atmosphere, along with sea surface temperature and surface currents in the ocean is described, and a difference with NAO phase is found. In positive NAO winters, an extension of the Gulf Stream warm core is observed, along with a displacement and acceleration of surface currents. Mesoscale activity in the atmosphere appears to follow this extension of the warm core of the Gulf Stream. This, we suggest, is a new feature of NAO air-sea interactions which is embedded within the basin-scale NAO patterns discussed previously in the literature. Further downstream, mesoscale activity seems to reflect more passively the general poleward migration of synoptic activity in positive NAO conditions.

1. Introduction

The leading mode of winter-to-winter climate variability in the North Atlantic basin consists in a meridional shift of the storm-track and associated wind, temperature, and precipitation patterns called the North Atlantic Oscillation (NAO; e.g., Hurrell et al., 2001). For example, cyclone tracking indicates a poleward shift of cyclones in positive compared to negative NAO conditions for both “extreme” and “nonextreme” cyclones (Pinto et al., 2009). It has been well established that the NAO exists independently of the presence of the underlying ocean (Thompson et al., 2003), although the changes associated with the NAO in air-sea heat fluxes and Ekman advection drive, on monthly time scales, a large-scale tripolar sea surface temperature (SST) anomaly pattern (e.g., Bjerknes, 1964; Frankignoul, 1985; Wallace et al., 1990). It has been suggested that this SST tripole is feeding back positively on the NAO (e.g., Czaja & Frankignoul, 2002) although this effect is weaker than the atmospheric forcing of the ocean (e.g., Kushnir et al., 2002).

On time scales longer than a few years, the geostrophic circulation of the North Atlantic Ocean also responds to the NAO, as was first suggested by Bjerknes (1964). Observations have shown that the Gulf Stream shifts poleward following a positive NAO phase (Taylor & Stephens, 1998; Frankignoul et al., 2001), and this result has been confirmed in numerical models (e.g., Sasaki & Schneider, 2011).

The studies cited above have dealt with fairly coarse atmospheric data sets, typically with a scale of several hundreds of kilometers. Recent studies with higher-resolution forecasting systems have emphasized that the wintertime NAO has a useful predictive skill and possibly more so in nature than in models (e.g., Dunstone et al., 2016). The recent release of the ERA5 data set (see below), as well as the improvement in resolution in SST data sets, makes it possible to start investigating whether smaller spatial scale signals, typically 100 km or less, are also part of the NAO and its interaction with the ocean. This is the focus of this study, with an emphasis on the wintertime period when the NAO and North Atlantic air-sea interactions are the strongest. The paper is organized as follows: Section 2 describes the data and methodology used for the analysis. Section 3 shows the spatial distribution of oceanic and atmospheric variables in ERA5 for different NAO phases, followed by discussion and conclusions in sections 4 and 5, respectively.

2. Data and Methodology

In this study, we use ERA5 reanalysis data (currently available from 2008 to present) which has a spatial resolution of 0.25° (<https://www.ecmwf.int/en/forecasts/datasets/archive-datasets/reanalysis-datasets/era5>). The period analyzed is December, January, and February, and positive and negative NAO years are selected when both the principal component and station NAO index agree on sign, based on Hurrell et al. (2003).

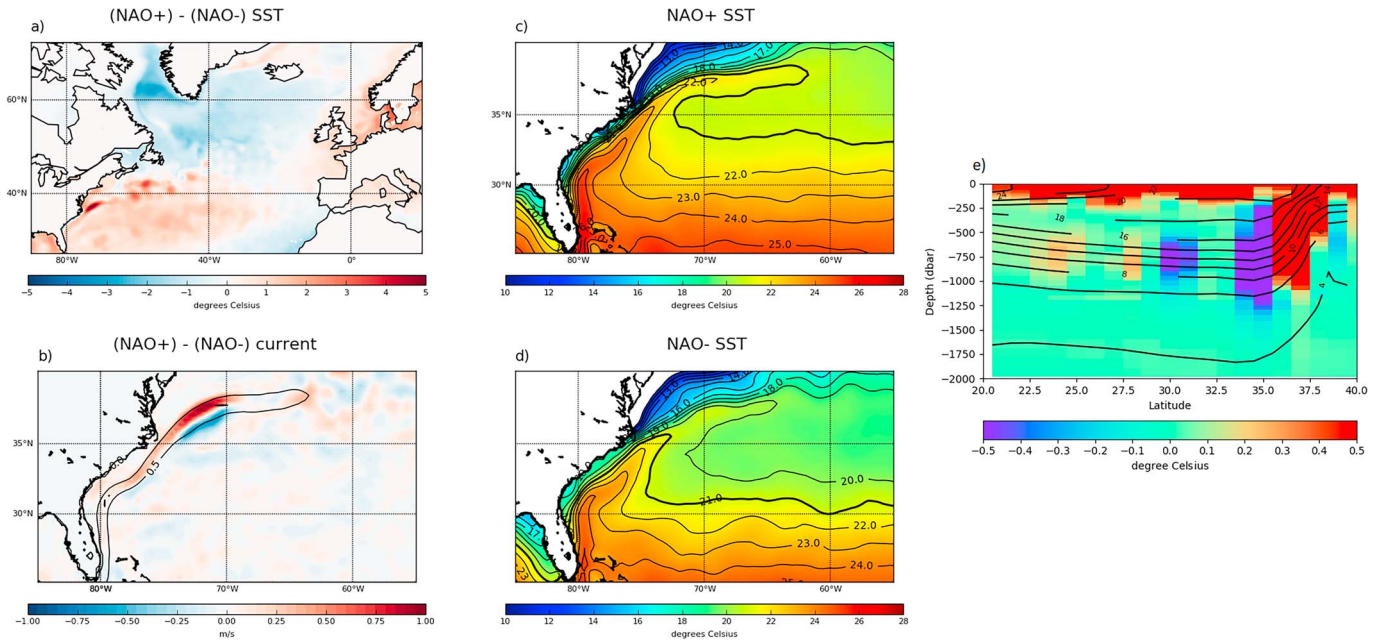


Figure 1. (a) Difference in SST between NAO+ and NAO-. SST in (c) NAO+ and (d) NAO- with 21 °C contour highlighted in bold. (b) Same as (a) but for surface currents (color). The contour line in (b) indicates a time mean current of 0.5 m/s. (e) Same as (a) but for potential temperature at 72.5° W (color). Black contours indicate the mean potential temperature ($c_i = 2$ K) from the Roemmich and Gilson climatology. For (a–d), NAO- winters are 2009–2010 and 2010–2011 and NAO+ are 2011–2012, 2013–2014, 2014–2015, 2015–2016, and 2016–2017. For (e), NAO- winters are 2009–2010 and 2010–2011 and NAO+ are 2011–2012, 2013–2014, and 2014–2015. All data averaged over December, January, and February. NAO = North Atlantic Oscillation; SST = sea surface temperature.

This results in five positive NAO winters (2011–2012, 2013–2014, 2014–2015, 2015–2016, and 2016–2017) and two negative NAO winters (2009–2010 and 2010–2011).

In this study, we emphasize spatial scales of a 100 km or less, which we broadly refer to in the following as “mesoscale.” Specifically, we focus on the high-pass filtered horizontal kinetic energy, hereafter referred to as mesoscale kinetic energy or *MKE*, defined as

$$MKE = \frac{\overline{u'^2 + v'^2}}{2}. \quad (1)$$

In this equation, the overline indicates a (coarse) spatial average and the primes departures from it, while (u, v) are the horizontal component of the velocity vector. *MKE* obeys an equation of the form Gaspar et al. (1990):

$$\frac{\partial}{\partial t} MKE = \text{Shear production} + \text{Buoyancy production} + \dots, \quad (2)$$

where

$$\text{Shear production} = - \left(\overline{\omega' u'} \cdot \frac{\partial \bar{u}}{\partial p} + \overline{\omega' v'} \cdot \frac{\partial \bar{v}}{\partial p} \right), \quad (3)$$

and

$$\text{Buoyancy production} = - \overline{\omega' \alpha'}. \quad (4)$$

In the above equations, we use pressure (p) coordinates, ω is the pressure vertical velocity, and α is specific volume. (Note that we have omitted the effect of large-scale advection and viscosity in (2).) Our aim is to evaluate how *MKE* and its buoyancy and shear production terms (BP and SP, respectively) vary according to NAO phases. To highlight the production of *MKE*, we will display in section 3 the average of BP and SP over the time records when these were found to be positive. The spatial filtering is based on a simple box average of size $\approx 3^\circ$ (analysis using a Lanczos filter produced very similar results, not shown). All calculations are

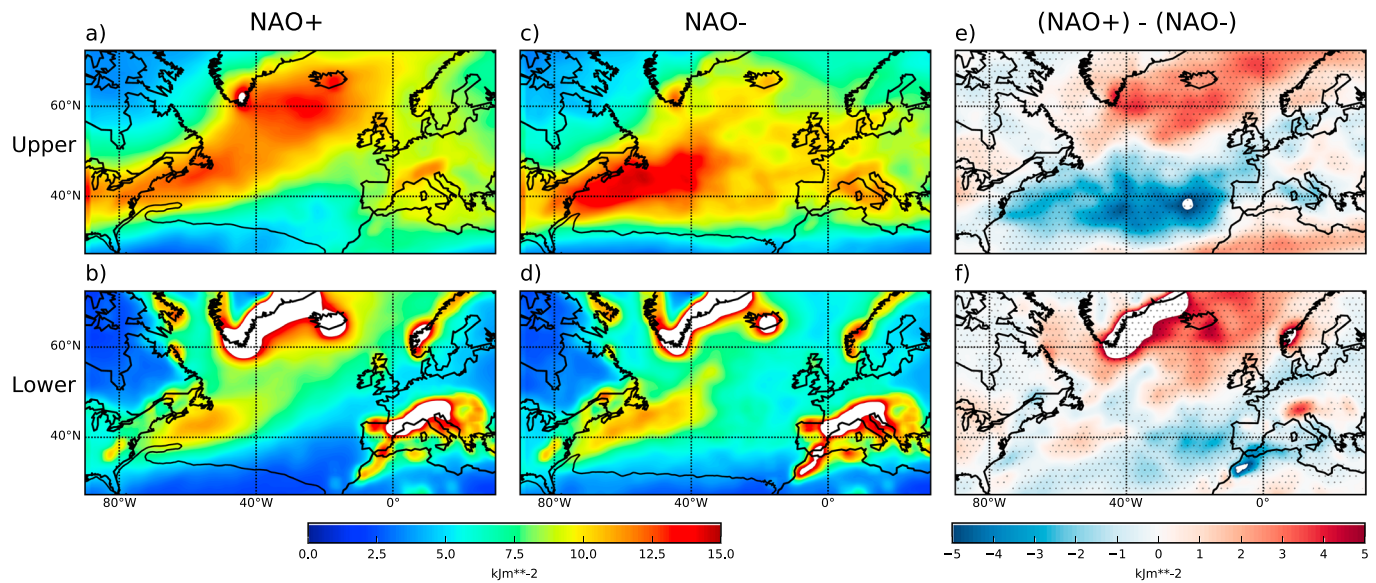


Figure 2. Distribution of mesoscale kinetic energy, (kilojoules per meter squared, kJm^{-2} , equation (1)), integrated over the upper atmosphere (300–600 hPa) in (a) NAO+ and (c) NAO– and the lower atmosphere (625–925 hPa) in (b) NAO+ and (d) NAO–. The difference between NAO+ and NAO– is displayed in (e) upper atmosphere and (f) lower atmosphere. Stippling indicating significance at the 95% level. The 21°C SST isotherm is shown in black contours in (a)–(d). At saturation, white is shown. NAO– winters are 2009–2010 and 2010–2011 and NAO+ are 2011–2012, 2013–2014, 2014–2015, 2015–2016, and 2016–2017. NAO = North Atlantic Oscillation.

performed on pressure levels, so u and v in equation (3) are isobaric components. Integration across levels 300–600 and 625–925 hPa are defined as upper and lower levels, respectively. All calculations shown in this study were performed using hourly data, but similar results were obtained using only 6-hourly data.

The SSTs in ERA5 (2008–present) are from the Operational Sea Surface Temperature and Sea Ice Analysis, which is provided on a regular grid of 0.05° resolution (Donlon et al., 2012). The Ocean Surface Current Analysis Real-time data set (Bonjean & Lagerloef, 2002) contains near-surface ocean current estimates, on a 0.33° grid at a 5-day temporal resolution.

Results for positive (NAO+) and negative (NAO–) NAO years are shown, as well as their difference. The significance of this difference is calculated using the t test of all hourly data points over the five NAO+ and two NAO– winters. Due to the decorrelation time scale of NAO, the number of degrees of freedom is reduced from the large number of hourly values. An NAO cycle is approximately 10 days (Feldstein, 2000), and so within the 90-day winter season, there is a maximum of nine independent cycles. To be conservative, this value has been halved (to 4); therefore, five NAO+ winters and two NAO– winters give 20 and 8 independent NAO, yielding 28 degrees of freedom.

3. Results

3.1. Mesoscale Signature in the Upper Ocean

Comparison of NAO+ and NAO– SSTs in ERA5 reveals the classic large-scale SST tripole, and embedded therein is a finer structure, with a maximum warming of 3°C in NAO+ to the east of Cape Hatteras (Figure 1a). The warm core of the Gulf Stream is narrower, warmer, and more extended toward the northeast in NAO+, as seen by comparison of the absolute SSTs in Figures 1c and 1d. Examination of surface currents shows that there is an acceleration along the axis of the warm core of the Gulf Stream and a northward shift in NAO+ compared to NAO– (Figure 1b). The mean surface current speed (contour line in Figure 1b) is 0.5 ms^{-1} and is comparable to the magnitude of the anomalies, suggesting a very significant change of the current. Analysis of meridional hydrographic sections from Argo data (Roemmich & Gilson, 2009) in the western North Atlantic in Figure 1e (color) shows a shallow signature of warmer water reflecting the warm part of the SST tripole but also a warm anomaly extending deeper to about a 1,000 m around 37°N . The collocation of this anomaly with the time mean temperature front (contours in Figure 1e) suggests that a poleward shift of the latter is responsible for the anomaly. In the following figures, the location of the 21°C isotherm at the sea surface will be used to track the extension of the separated Gulf Stream.

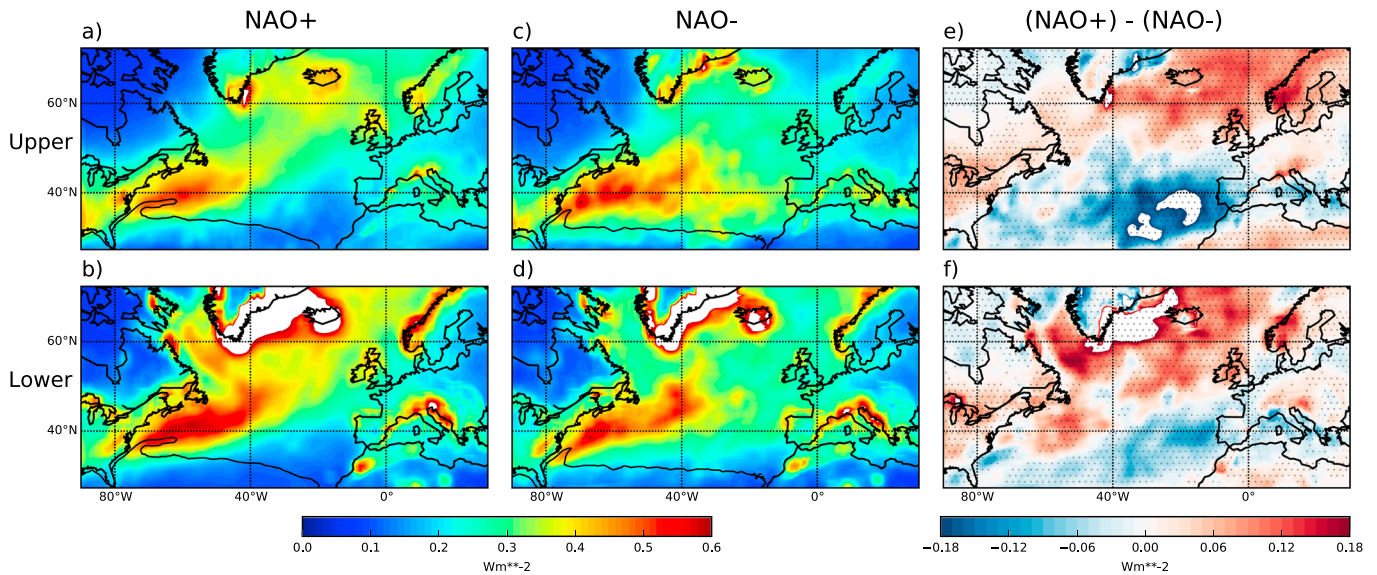


Figure 3. Same as Figure 2 but for the production of *MKE* by buoyancy effects, see equation (4), in units of watts per meter squared (Wm^{-2}). Note that this time averages over records where $BP > 0$.

3.2. Mesoscale Signature in the Atmosphere

The distribution of *MKE* at upper and lower levels for positive and negative NAO winters, as well as their difference, is displayed in Figure 2. At upper levels (top panels), one observes an enhancement of *MKE* activity centered at 60° N in NAO+ (Figure 2a), while this feature is more restricted to 45° N in NAO- (Figure 2c). This reflects the expected poleward displacement of the synoptic systems with NAO (e.g., Pinto et al., 2009) and is clearly visible in the meridional dipole structure centered at 50° N in Figure 2e. A similar feature is also seen at lower levels (bottom panels), but note, in addition, the presence of a southwest to northeast oriented dipole near the Gulf Stream in Figure 2f.

To investigate the cause of these features, we display the production of *MKE* by buoyancy (Figure 3) and shear (Figure 4) effects. At upper levels, one recovers the north-south shift (Figures 3e and 4e). This suggests that as the synoptic systems shift poleward in NAO+ so does the mesoscale activity production embedded in them.

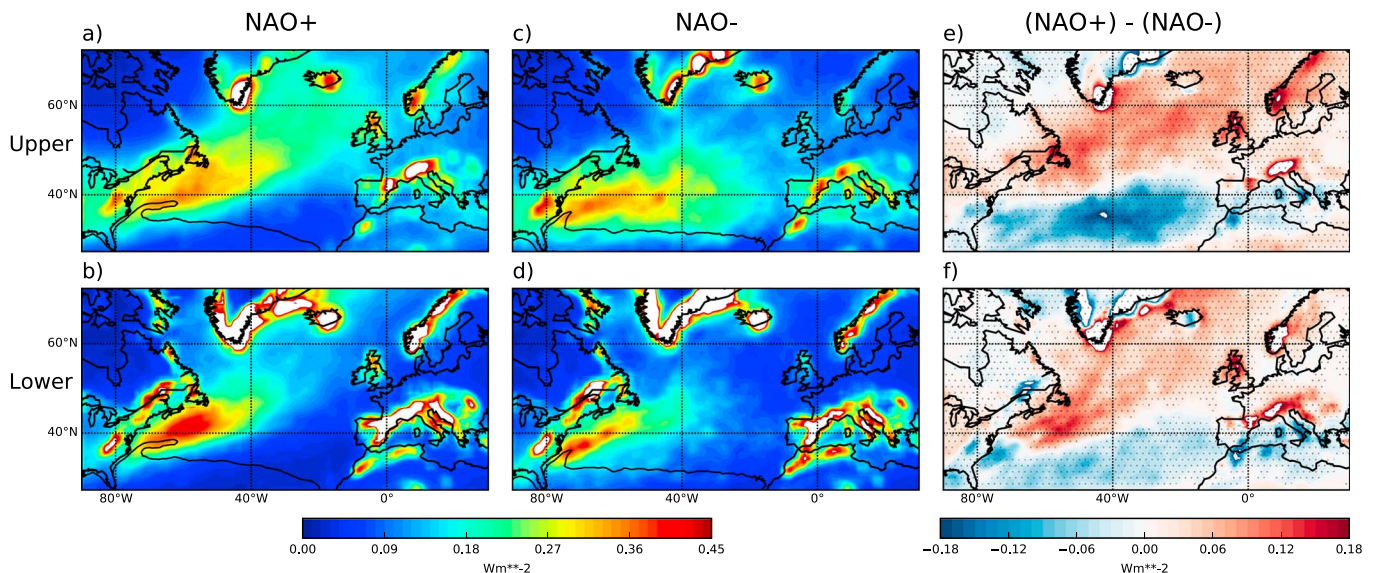


Figure 4. Same as Figure 2 but for the production of *MKE* by shear effects, see equation (3), in units of watts per meter squared (Wm^{-2}). Note that this time averages over records where $SP > 0$.

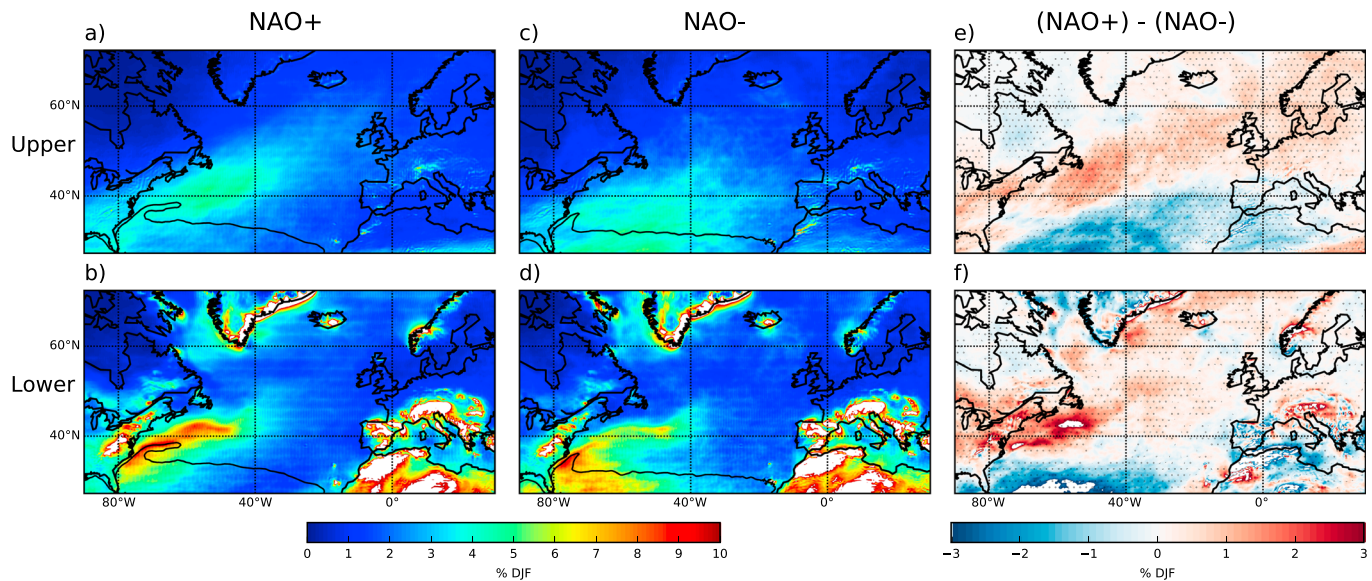


Figure 5. As in Figure 2 but for the frequency (percentage of December, January, and February) of occurrence of $PV < 0$. The t test applies to the mean of a binary variable derived from PV (1 when negative, 0 otherwise), not the PV itself.

The lower level composites recover this feature but also highlight the presence of the southwest-northeast dipole mentioned above, this dipole being particularly pronounced in the shear production composite (Figure 4f). Inspection of scatter plots between MKE and BP , SP , and $BP + SP$ suggest a stronger relationship between these in $NAO+$ compared to $NAO-$ (not shown). Scatter plots for the $(NAO+)-(NAO-)$ composite support the view that the southwest-northeast dipole signal in MKE is a result of the localization of the production terms at low levels, with a correlation coefficient of 0.71 significant at the 95% level for the sum $BP + SP$ versus MKE scatter plot. Interestingly, the signs of this dipole are such that when the separated Gulf Stream is more extended, the mesoscale activity is shifted to the northeast, while it is more limited to the southwest part of the basin when the separated Gulf Stream is itself less extensive (see the location of the production terms with respect to the 21 °C isotherm in Figures 3b, 3d, 4b, and 4d). This suggests an anchoring of the production of MKE by the Gulf Stream, a distinct feature from the large-scale poleward shift dominating the upper-level composites. This, we suggest, is a new mesoscale structure of air-sea interactions associated with the NAO.

The localization of mesoscale activity by the Gulf Stream is further supported by an inspection of the Ertel potential vorticity (PV) field (Figure 5, displaying the frequency of occurrence of events with $PV < 0$). In a 2-D flow in thermal wind balance, $PV < 0$ is known as a signature of instability (e.g., Bennetts & Hoskins, 1979) and so provides an alternative view to the shear production term in Figure 4. ERA5 outputs PV on pressure levels, from which negative values are counted and then averaged over the upper and lower levels, so 10% of negative frequency means that 10% of hourly data within the level bounds has $PV < 0$. The frequency of these events is larger at lower than at upper levels and is about 5% to 10%. The spatial distribution confirms the view from Figures 3 and 4 that upper levels are dominated by the north-south shift of the storm track but with an additional signal in the western Atlantic at low levels: A more pronounced northward extension of occurrence of $PV < 0$ events when the separated Gulf Stream is more extended ($NAO+$, Figure 5b), and a more limited occurrence of these events north of 40° N ($NAO-$, Figure 5d) when the warm water core of the Gulf Stream is more confined to the American coast.

Finer analysis of the vertical dependence of the signals in Figure 5 indicates that the high frequency of negative PV events in the lower levels is dominated by that at 925 hPa (not shown). This is consistent with Vanni re et al. (2016) who showed that southeastward advection of continental air over the ocean by a cyclone in a cold air outbreak produces $PV < 0$ near the sea surface with a frequency comparable to that of cold fronts (5–10%). Throughout the rest of the troposphere, the frequency of events with $PV < 0$ is consistently lower but with a relative increase at the 300 hPa (not shown). This is expected if strong updrafts carry the $PV < 0$ air mass from the boundary layer to these levels and then subsequently spread it nearly

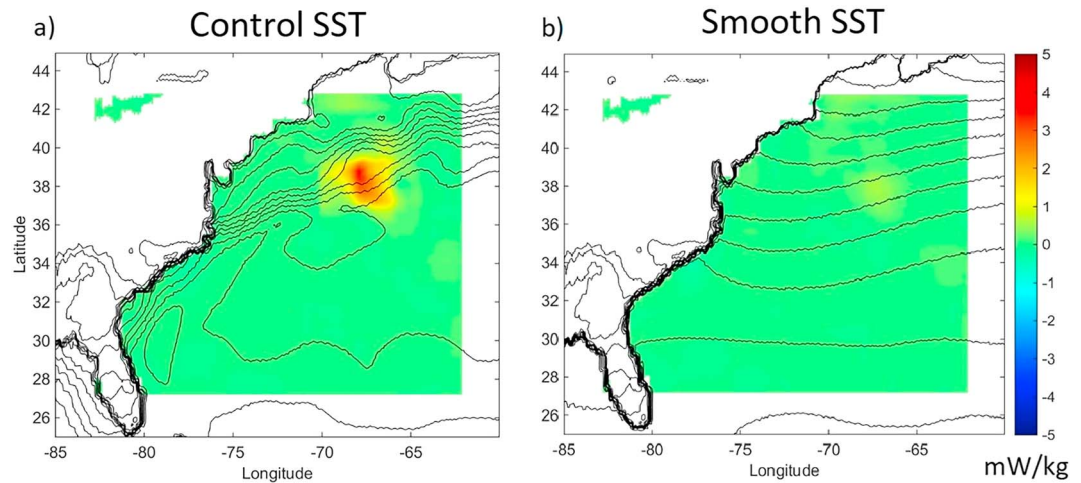


Figure 6. Distribution of shear production (color)—see equation (3)—at a height of 4.5 km, 24 hr into the model simulation by Sheldon et al. (2017), (a) Control SST and (b) Smoothed SST. The associated SST distributions are shown in black contours with a contour interval of 2K. SST = sea surface temperature.

horizontally. Both positive and negative changes in PV are expected from latent heat release during ascent, but the net effect of these is smaller ($\approx +0.1 PVU$, see Madonna et al., 2014) than the initial negative PV near the surface ($\approx -1 PVU$, see Vanni re et al., 2016).

4. Discussion

The results presented above are admittedly based on a limited sample size due to the current availability of the ERA5 data set. To test their robustness, we have repeated the analysis with ERA-Interim 6-hourly data (1979–present; Dee et al., 2011), allowing us to consider 20 NAO+ and 13 NAO– winters. To be consistent, the “bar” term in equations (2)–(4) was set to cover the same area as in ERA5, but because of the coarser resolution in ERA-Interim, the “prime” term now represents at most scales of 0.75° as opposed to 0.25° in ERA5. Results over the 1979–2017 period reveal the same large-scale poleward signal associated with storm track in NAO+ compared to NAO–, as well as the more localized signal over the Gulf Stream region (not shown). As in ERA5, the latter is clearly seen at lower levels although with half the magnitude. Thus, we are confident that this localized feature is robust. Interestingly, comparison of upper and lower panels in Figure S1 indicates that this feature only showed up clearly after 2002, which is when the resolution of the SST data used in ERA-Interim was improved (first in January 2002 from 1° , Reynolds et al., 2002, to 0.5° , Thi baux et al., 2003, and then again in February 2009 to 0.05° , Donlon et al., 2012).

The southwest-northeast dipole just discussed is most readily seen at lower levels in Figures 3–5, but a finer analysis of pressure levels indicates that it is also present at upper levels (see the discussion of PV maps in section 3.2). Indeed, it is a distinct feature from the “surface storm-track” related to the Gulf Stream and discussed in Booth et al. (2010) with a much coarser data set (1.125° for 10-m winds and 2.5° for 850-hPa winds).

We have linked empirically periods when the Gulf Stream warm core is more extended northeastward to a similar extension of MKE and its production terms. The study by Sheldon et al. (2017), as well as the difference in ERA-Interim composites with SST resolution noted above give support for the view that this relationship is causal. In Figure 6, we show the shear production term at 4.5-km height in the case study considered by Sheldon et al. (2017) when the SST was realistic (left panel) and when it was heavily smoothed, thereby removing the SST signature of the Gulf Stream (right panel). Comparison of the two panels shows that in this particular experiment (UK Met Office model at 12-km horizontal resolution—see Sheldon et al., 2017, for details), the presence of the Gulf Stream warm core sets a region of positive shear production of MKE downstream of it. It is tempting to interpret the localized southwest-northeast dipole in Figure 4f as evidence in the climatology of the signal seen in a single storm in Sheldon et al. (2017). More modeling work is clearly needed to test this hypothesis fully.

5. Conclusions

The results of our analysis can be summarized as follows:

- Composite analysis for SST, surface current, and subsurface temperature reveals a northeastward shift of the Gulf Stream and extension of its warm core in NAO+ winters compared to NAO-. A similar analysis for spatially high-pass filtered atmospheric quantities (mesoscale) indicates that, in addition to the large-scale meridional shift of the storm track previously documented in NAO studies, there is a more localized or “mesoscale signal” tied to the movement of the Gulf Stream.
- The analysis above, although based on a short record with ERA5, is reproduced in the longer ERA-Interim data set, albeit with a weaker magnitude.

We have suggested that the new mesoscale NAO signal highlighted in this study is reflecting a forcing of the atmosphere by the ocean, as opposed to the more dominant atmospheric forcing of the SST tripole on large (basin) spatial scale. This hypothesis, and whether this mesoscale signal can affect the storm track and its variability further downstream, remains to be investigated in future work.

Acknowledgments

Alison Cobb was funded by a PhD studentship from the Grantham Institute at Imperial College London. We acknowledge ERA5, ERA-Interim, OSCAR, and Argo (Roemmich and Gilson climatology) for data sets and Magdalena Balmaseda and Frederic Vitart at ECMWF for useful discussions. Access of ERA5 from the Copernicus Climate Change Service Climate Data Store (CDS; <https://cds.climate.copernicus.eu/#!/search?text=ERA5&type=dataset>), ERA-Interim (<https://apps.ecmwf.int/datasets/data/interim-full-daily/levtype=sfc/>), OSCAR (<https://doi.org/10.5067/OSCAR-03D01>), and Argo (http://sio-argo.ucsd.edu/RG_Climatology.html).

References

- Bennetts, D., & Hoskins, B. (1979). Conditional symmetric instability—A possible explanation for frontal rainbands. *Quarterly Journal of the Royal Meteorological Society*, *105*(446), 945–962.
- Bjerknes, J. (1964). Atlantic air-sea interaction. In *Advances in geophysics* (Vol. 10, pp. 1–82): Elsevier.
- Bonjean, F., & Lagerloef, G. S. (2002). Diagnostic model and analysis of the surface currents in the tropical Pacific Ocean. *Journal of Physical Oceanography*, *32*(10), 2938–2954.
- Booth, J. F., Thompson, L. A., Patoux, J., Kelly, K. A., & Dickinson, S. (2010). The signature of the midlatitude tropospheric storm tracks in the surface winds. *Journal of Climate*, *23*(5), 1160–1174.
- Czaja, A., & Frankignoul, C. (2002). Observed impact of Atlantic SST anomalies on the North Atlantic Oscillation. *Journal of Climate*, *15*(6), 606–623.
- Dee, D. P., Uppala, S., Simmons, A., Berrisford, P., Poli, P., Kobayashi, S., et al. (2011). The ERA-Interim reanalysis: Configuration and performance of the data assimilation system. *Quarterly Journal of the Royal Meteorological Society*, *137*(656), 553–597.
- Donlon, C. J., Martin, M., Stark, J., Roberts-Jones, J., Fiedler, E., & Wimmer, W. (2012). The Operational Sea Surface Temperature and Sea Ice Analysis (OSTIA) system. *Remote Sensing of Environment*, *116*, 140–158.
- Dunstone, N., Smith, D., Scaife, A., Hermanson, L., Eade, R., Robinson, N., et al. (2016). Skilful predictions of the winter North Atlantic Oscillation one year ahead. *Nature Geoscience*, *9*(11), 809.
- Feldstein, S. B. (2000). The timescale, power spectra, and climate noise properties of teleconnection patterns. *Journal of Climate*, *13*(24), 4430–4440.
- Frankignoul, C. (1985). Sea surface temperature anomalies, planetary waves, and air-sea feedback in the middle latitudes. *Reviews of Geophysics*, *23*(4), 357–390.
- Frankignoul, C., de Coëtlogon, G., Joyce, T. M., & Dong, S. (2001). Gulf Stream variability and ocean-atmosphere interactions. *Journal of Physical Oceanography*, *31*(12), 3516–3529.
- Gaspar, P., Grégoris, Y., & Lefevre, J.-M. (1990). A simple eddy kinetic energy model for simulations of the oceanic vertical mixing: Tests at station Papa and long-term upper ocean study site. *Journal of Geophysical Research*, *95*(C9), 16,179–16,193.
- Hurrell, J. W., Kushnir, Y., Ottersen, G., & Visbeck, M. (2003). *An overview of the North Atlantic oscillation* (pp. 1–35). American Geophysical Union.
- Hurrell, J. W., Kushnir, Y., & Visbeck, M. (2001). The North Atlantic Oscillation. *Science*, *291*(5504), 603–605.
- Kushnir, Y., Robinson, W., Bladé, I., Hall, N., Peng, S., & Sutton, R. (2002). Atmospheric GCM response to extratropical SST anomalies: Synthesis and evaluation. *Journal of Climate*, *15*(16), 2233–2256.
- Madonna, E., Wernli, H., Joos, H., & Martius, O. (2014). Warm conveyor belts in the ERA-Interim dataset (1979–2010). Part I: Climatology and potential vorticity evolution. *Journal of Climate*, *27*(1), 3–26.
- Pinto, J. G., Zacharias, S., Fink, A. H., Leckebusch, G. C., & Ulbrich, U. (2009). Factors contributing to the development of extreme North Atlantic cyclones and their relationship with the NAO. *Climate Dynamics*, *32*(5), 711–737.
- Reynolds, R. W., Rayner, N. A., Smith, T. M., Stokes, D. C., & Wang, W. (2002). An improved in situ and satellite SST analysis for climate. *Journal of Climate*, *15*(13), 1609–1625.
- Roemmich, D., & Gilson, J. (2009). The 2004–2008 mean and annual cycle of temperature, salinity, and steric height in the global ocean from the Argo Program. *Progress in Oceanography*, *82*(2), 81–100.
- Sasaki, Y. N., & Schneider, N. (2011). Interannual to decadal Gulf Stream variability in an eddy-resolving ocean model. *Ocean Modelling*, *39*(3–4), 209–219.
- Sheldon, L., Czaja, A., Vannièrè, B., Morcrette, C., Sohet, B., Casado, M., & Smith, D. (2017). A ‘warm path’ for Gulf Stream-troposphere interactions. *Tellus A: Dynamic Meteorology and Oceanography*, *69*(1), 1299397.
- Taylor, A. H., & Stephens, J. A. (1998). The North Atlantic Oscillation and the latitude of the Gulf Stream. *Tellus A*, *50*(1), 134–142.
- Thiébaux, J., Rogers, E., Wang, W., & Katz, B. (2003). A new high-resolution blended real-time global sea surface temperature analysis. *Bulletin of the American Meteorological Society*, *84*(5), 645–656.
- Thompson, D. W., Lee, S., & Baldwin, M. P. (2003). Atmospheric processes governing the northern hemisphere annular mode/North Atlantic Oscillation. *Geophysical Monograph-American Geophysical Union*, *134*, 81–112.
- Vannièrè, B., Czaja, A., Dacre, H., Woollings, T., & Parfitt, R. (2016). A potential vorticity signature for the cold sector of winter extratropical cyclones. *Quarterly Journal of the Royal Meteorological Society*, *142*(694), 432–442.
- Wallace, J. M., Smith, C., & Jiang, Q. (1990). Spatial patterns of atmosphere-ocean interaction in the northern winter. *Journal of Climate*, *3*(9), 990–998.